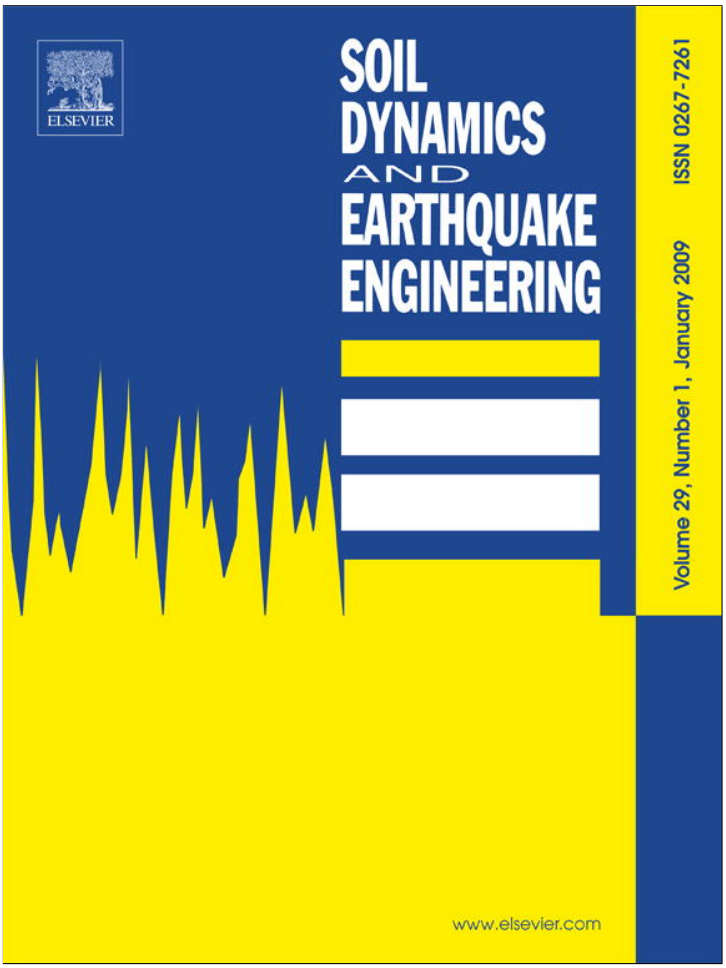

ELSEVIER

Soil Dynamics and Earthquake Engineering 29 (2009) 133–143

SOIL DYNAMICS AND EARTHQUAKE ENGINEERING

www.elsevier.com/locate/soildyn

Comparison of three different methods in investigating shallow shear-wave velocity structures in Ilan, Taiwan

Chun-Hsiang Kuo[a], Ding-Shing Cheng[b], Hung-Hao Hsieh[c], Tao-Ming Chang[c], Hsien-Jen Chiang[a], Che-Min Lin[a], Kuo-Liang Wen[a,*]

[a]*Institute of Geophysics, National Central University, No. 300, Jhongda Road, Jhongli City, Taoyuan County 32001, Taiwan*
[b]*Department of Enviromental Information and Engineering, Chung Cheng Institute of Technology, National Defense University, Taoyuan, Taiwan*
[c]*National Center for Research on Earthquake Engineering, Taipei, Taiwan*

Received 3 July 2007; received in revised form 15 November 2007; accepted 17 January 2008

Abstract

The Central Weather Bureau (CWB) and National Center for Research on Earthquake Engineering (NCREE) launched a project to build an engineering geological database for strong-motion stations in Taiwan in 2000. The project measures shear-wave velocity using the suspension PS-logging method. In this study, we conduct array measurements of microtremors and apply the stress wave propagation method (SWPM) at seven free-field strong-motion stations in Ilan County to estimate shallow shear-wave velocity structures. We focus on the sediment layers of the top 100 m to compare the shear-wave velocity structures of the three different methods. There are some misfits among the results of the three different methods; so we calculate the values of Vs_{30}, Vs_{100} and plot S-wave travel-time curves of these methods for each site to analyze the misfits effectively. This analysis helped us to prove the efficiency of the microtremor array method in investigating shear-wave velocity structures in the shallow subsurface. Moreover, the horizontal-to-vertical ratios of microtremors for each survey point show the existence of divergence at the same site. We considered this as evidence that misfits are caused by the heterogeneous nature of sediments and also due to the nature of the methods as being one-, two- and three-dimensional. Furthermore, the average shear-wave velocity structure of microtremor arrays may be more representative of the whole site.

Keywords: Microtremor array; PS-logging; Stress wave propagation method (SWPM)

1. Introduction

Determination of shear-wave velocity structure is very important in theoretical simulation and strong ground motion prediction, especially for the sedimentary cover of bedrock. There are many methods used to evaluate subsurface shear-wave velocity structure, and in this study we conduct three such methods for comparative purposes; they are the array measurement of microtremors, suspension PS-logging and the stress wave propagation methods (SWPM). Some studies have used the microtremor array method to evaluate shallow velocity structures (<300 m), and compared their results with borehole data or reflection profiles (e.g. [1–7]). Mostly, the comparative data were collected at a large distance (more than 1 km) from the microtremor array (e.g. [3]). There have also been studies which compared microtremor arrays and PS-logging results from nearby boreholes and these were considered more credible (e.g. [4–7]). And there has been some research containing PS-logging and the spectral analysis of surface waves (SASW) results, but two such measurements are separately at two sites (e.g. [8]).

In the past, we have conducted array measurements of microtremor in several tens of free-field strong-motion stations to estimate shallow shear-wave velocity structures. In addition, at these same stations, velocity structures were also investigated using the SWPM. In 2000, the Central Weather Bureau (CWB) and National Center for Research on Earthquake Engineering (NCREE) of Taiwan launched a project to build an engineering geological database for strong-motion stations and measured shear-wave velocity

*Corresponding author. Tel.: +886 3 4260955; fax: +886 3 4222044.
E-mail address: wenkl@earth.ncu.edu.tw (K.-L. Wen).

0267-7261/$ - see front matter © 2008 Elsevier Ltd. All rights reserved.
doi:10.1016/j.soildyn.2008.01.010

using the suspension PS-logging method. The SWPM is an augmented method that combines the spectral analysis of surface waves (SASW) and the impulse response (IR) methods. The SASW method is known for its accuracy in determining the shear-wave velocity structure of the shallow subsurface (e.g. [9,10]) and the PS-logging method is a kind of direct measurement used within boreholes. In this study, we compared the results of these three different methods, microtremor array, SWPM and PS-logging, at seven selected sites distributed though out Ilan County. The results of the three different methods are very similar for most sites, so we can reasonably speculate that the microtremor array method is also an effective tool for exploring shear-wave velocity structure in the shallow subsurface.

The seven sites are all located in elementary schools; consequently, the measurements were all conducted during summer vacation in order to avoid artificial noise inside the array and to increase the convenience of field works. In this paper, we focus on shallow shear-wave velocity structures at a depth of about 0–50 or 100 m. The SWPM and PS-logging method are considered efficient methods for estimating shallow sedimentary shear-wave velocity structures, but typically the microtremor array method is used to evaluate deep shear-wave velocity structures at depths ranging from hundreds of meters to several kilometers depending on the array's diameter [11]. In other words, to date, there have been very few studies utilizing microtremor array measurement focusing on shear-wave velocity structures of the uppermost subsurface, i.e. at a depth of less than 100 m. Consequently, one of the goals of this study is to assess the feasibility and accuracy of the microtremor array method in determining shear-wave velocity structures in the top 100 m of the subsurface through comparison with the velocity structures resulting from PS-logging and SWPM.

2. Measurements of three different methods

The seven selected sites are distributed in Ilan, including ILA003, ILA005, ILA013, ILA029, ILA041, ILA042, and ILA044. Fig. 1 shows the locations of these sites: all are on an alluvium plain.

Our microtremor array measurements were completed using portable instruments—Tokyo Sokushin portable servo seismometers. A set of instrument includes a recorder SAMTAC-801B and a sensor VSE315D. The SAMTAC-801B is a 24-bit recorder with a MO access device, and the VSE315D is a six-channel seismometer with flat amplitude from 0.1 to 50 Hz as illustrated in Fig. 2. The internal clock was corrected by the global positioning system (GPS) before each measurement so that the systems could make simultaneous observations. The observation times for ILA003, ILA029, ILA041, ILA042, and ILA044 were 75 min with ten sets of portable seismometers in a triple circle array. Two arrays called small and large triple circle arrays were both installed in ILA005 and ILA013, had the same center but different radii, and thus two sets of 37-min

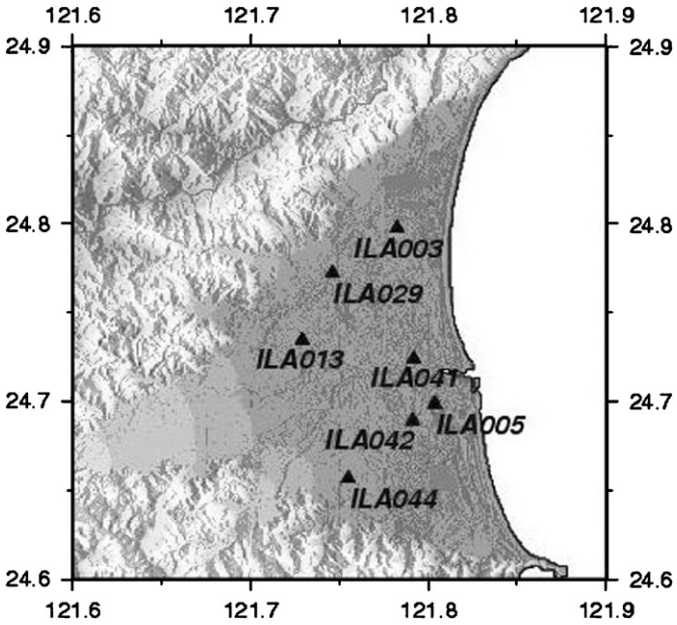

Fig. 1. The topography of Ilan with the station locations in this study. All sites are located in the Quaternary alluvial deposits.

observations for small and large arrays were performed, respectively. The sampling rate of all observations is 100 points per second. Fig. 3 shows examples of instrument locations, and the correlative parameters of microtremor array measurements are shown in Table 1.

In the SWPM experiments, we set two PCB383B12 accelerometers at different distances from each other and beat on the ground with a PCB086D50 hammer to produce a transient artificial source. The distances between the accelerometers were 2, 4, 8, 16 and 32 m at each site.

The logging depth at all sites was more than 30 m, except for ILA013 and ILA044. Furthermore, at sites ILA003 and ILA041 the lodging depth was even deeper at than 100 m. The P-wave and S-wave velocities were measured continuously at different depths with a suspension PS-logger from bottom to top. Because of the suspension PS-logger's limitations, measurements of shear-wave velocity in the top 2 or 3 m were unavailable. We measured shear-wave velocity every 0.5 m at ILA003, ILA005, ILA029, ILA041, and ILA042, and at the shallower sites of ILA013 and ILA044 measurements were conducted per meter.

3. Data analysis

3.1. Microtremor array

3.1.1. Frequency–wavenumber (F–K) method

In the late 1950s, Aki [12] proposed analysis of seismic noise as a good tool for investigating shear-wave velocity structures. He utilized small-scale seismic arrays and derived the phase-velocity dispersion curve by correlating noise records. Capon [13] proposed the maximum likelihood (high-resolution method) of frequency–wavenumber (*F–K*) method to determine the vector velocity of

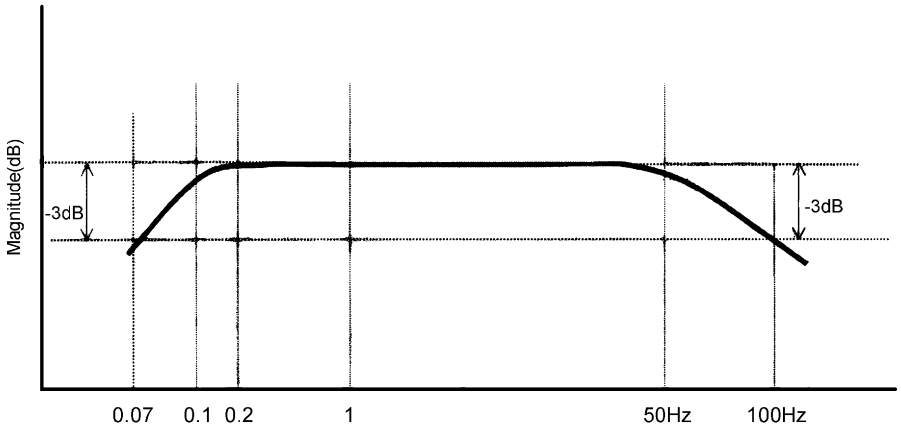

Fig. 2. This illustration shows the amplitude of the VSE315D sensor used in this study.

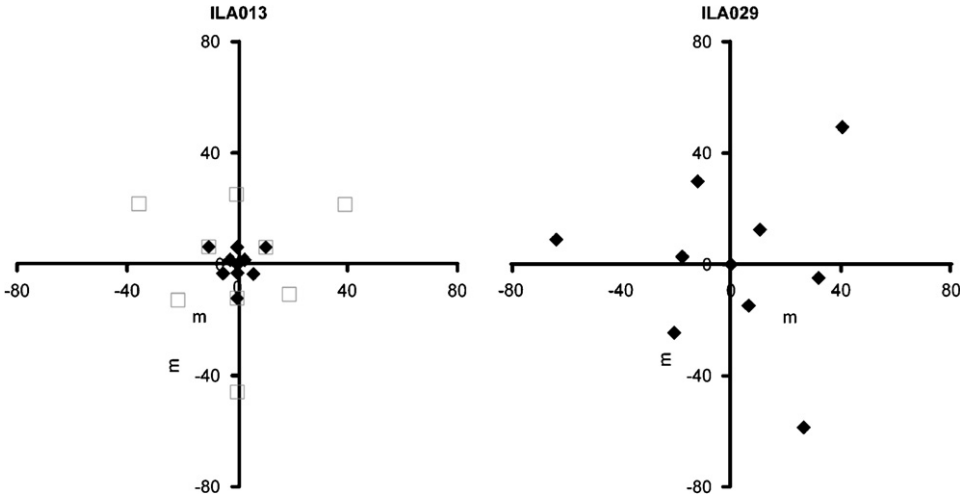

Fig. 3. Here were examples of the instruments' layouts. To the left is the site ILA013 and on the right is ILA029. The open square formation is the large array and the diamonds represent the small array at ILA013. The large and small arrays have the same center. ILA029 has only one array.

Table 1
Parameters of microtremor array measurements

Site	R_{min} (m)	R_{max} (m)	Measured time	Sampling rate
ILA003	8.1	32.2	75	100
ILA005	4.1	60.9	37 + 37	100
ILA013	3.1	45.9	37 + 37	100
ILA029	16.1	64.3	75	100
ILA041	8.1	32.2	75	100
ILA042	16.1	64.2	75	100
ILA044	16.1	64.1	75	100

Radii of each triple circle array were determined by the condition in situ; thus, the radii were not identical even in the same circle. R_{min} means the minimum radius and R_{max} indicates the maximum in meters. There are two triple circle arrays in ILA005 and ILA013 that we conducted two sets of 37 min measurements, nevertheless 75 min in other sites. Sampling rate in this study was unified to 100 points per second.

propagating seismic waves of large aperture seismic arrays (LASA), a method that provides seismic data for facilitating the discrimination between earthquakes and underground nuclear explosions. Hereafter, a Rayleigh wave inversion technique using array records of microtremors is proposed as a useful exploration method for obtaining the shear-wave velocity structures of sedimentary layers. The array exploration method of microtremors was established by Horike [14] and Matsushima and Okada [15] after the pioneering work done by Aki [12]. They used long-period microtremors to estimate deep shear-wave velocity structures. After that, Sato et al. [16] and Malagnini et al. [17] used short-period microtremors to estimate the shear-wave structures of shallow layers. Recently, Kawase et al. [18] and Satoh et al. [11] succeeded in estimating shallow and deep shear-wave velocity structures at several sites in America and the Sendai Basin in Japan using both short- and long-period microtremors. However, this method is based on the assumption that microtremors are dominated by the Rayleigh wave and the structures of measured sites are not sharply varying in the horizontal.

In the microtremor array method, natural surface vibrations are recorded by ten recorders, which are roughly arranged in an array of three concentric circles because we must avoid the buildings and culverts in school. The spatial

autocorrelation (SPAC) method and the *F–K* method are two techniques widely used in obtaining the phase velocities from microtremor array measurements. During field work, it must install stations equally spaced on a circle, one in the center and total seven at least when using the SPAC method [19]. However, we can install an arbitrarily shaped array for the *F–K* method and this is the reason why we use the *F–K* method in this study. *F–K* analysis is used to identify the dispersion curve of soil layers with only the vertical component of microtremor waveform data. By using the *F–K* method, we obtain the *F–K* spectra of various frequencies; these indicate the phase velocities of those frequencies. We use the vertical component derived from the observed records with window lengths of 512, 1024, 2048, 4096, and 8192 points by moving the window 200 points a time. After this, we perform a cross-correlation of each record of the same array to increase the signal to noise ratio and then conduct a 2D Fourier transform under the maximum likelihood method to obtain the *F–K* spectra. Here, we will briefly explain the *F–K* spectral analysis based on the maximum likelihood method [13]. In the assumption that the data $d_{i,t}$ in station i is composed of signal $S_{i,t}$ and noise $n_{i,t}$, then we can write data d_i as $d_{i,t} = S_{i,t}+n_{i,t}$, where $i = 1, \ldots, N$ and t is the discrete time. If time is the same, $d_i = S+n_i$, where $i = 1, \ldots, N$. Assume d_i conforms to a Gaussian distribution, and its mean value is S, then the covariance matrix can be written as $R_{i,j} = \langle n_i\, n_j \rangle$, and

$$F(d_i \ldots d_N) = \frac{|\phi|^{1/2}}{(\pi/2)^{N/2}} \exp\left[-\frac{\pi}{2}\sum_{i,j=1}^{N} \phi_{ij}(d_i - S)(d_j - S)\right] \tag{1}$$

Eq. (1) is called the joint probability density function, where ϕ_{ij} is the inverse matrix of $R_{i,j}$, and ϕ is the value of ϕ_{ij}.

In order to obtain a better signal, we hope that the value of $\sum_{i,j=1}^{N} \phi_{ij}(d_i - S)(d_j - S)$ is the minimum. We can obtain the differential of Eq. (1) in the following:

$$S = \frac{\sum_{j=1}^{N} \phi_{ij}}{\sum_{i,j=1}^{N} \phi_{ij}} d_i, \quad i = 1, \ldots, N \tag{2}$$

Eq. (2) is the weighting of each station and is directly proportional to ϕ_{ij}.

Capon [13] performed the maximum likelihood method to obtain the *F–K* spectra utilizing the previous method and got

$$P(k_x, k_y, \omega) = \left\{\sum_{i=1}^{N}\sum_{j=1}^{N} \phi_{ij}(\omega) \exp[\mathrm{i}k_x(x_i - x_j) + \mathrm{i}k_y(y_i - y_j)]\right\}^{-1} \tag{3}$$

We also checked the horizontal-to-vertical (H/V) spectra to make sure that the fluctuations of the H/V spectra were in agreement. The vertical components of microtremors and H/V spectra are shown in Fig. 4. Fig. 5 shows the examples of *F–K* spectra at frequencies of 2 and 5 Hz. Fig. 6 shows the dispersion curves of each site in this study.

3.1.2. Genetic algorithm (GA)

With the GA a search area was defined both for the velocity and the thickness of the layers. An initial

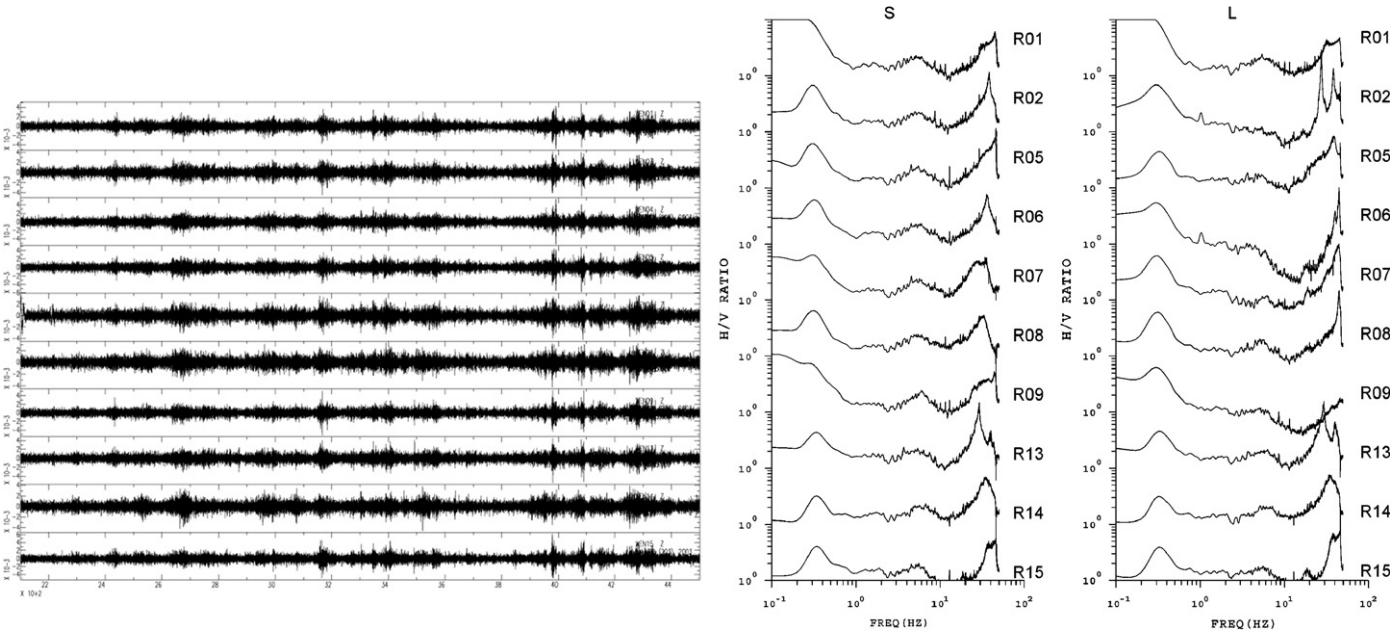

Fig. 4. Here are the vertical components of microtremor waveform data at ILA042 and the horizontal-to-vertical spectra at ILA005. "S" and "L" denote the spectra of the small and large arrays at ILA005. Rxx to the right of each spectrum denotes the instrument number. The higher amplification in frequencies lower than 0.3 Hz of R01 and R09 is caused by instrument effect.

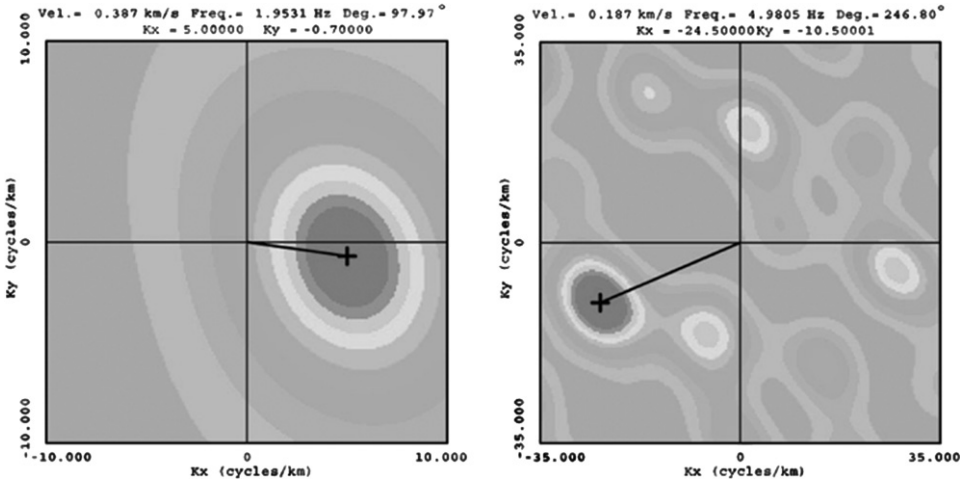

Fig. 5. The *F–K* spectra in the frequencies of 2 Hz (left) and 5 Hz (right) of ILA041. "Vel." is the phase velocity in km/s; "Freq." is the frequency in Hz; "Deg." gives the propagation direction clockwise from the north by degree; "K*x*" and "K*y*" give the wavenumber in the *x* and *y* directions, respectively.

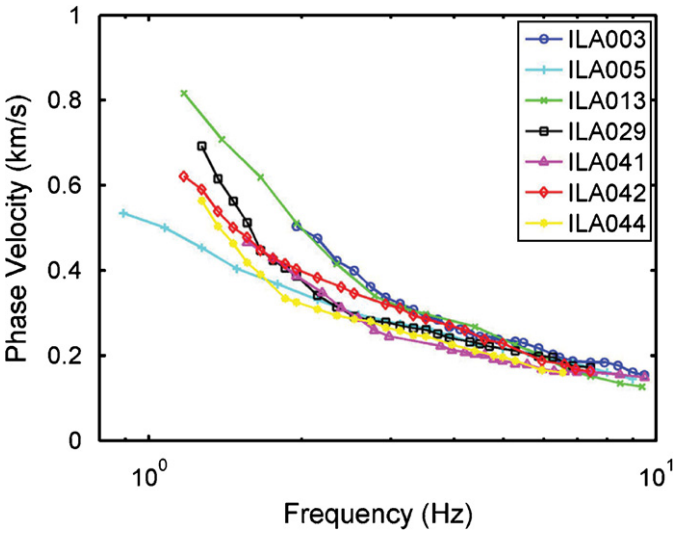

Fig. 6. The dispersion curves of the seven sites in this study.

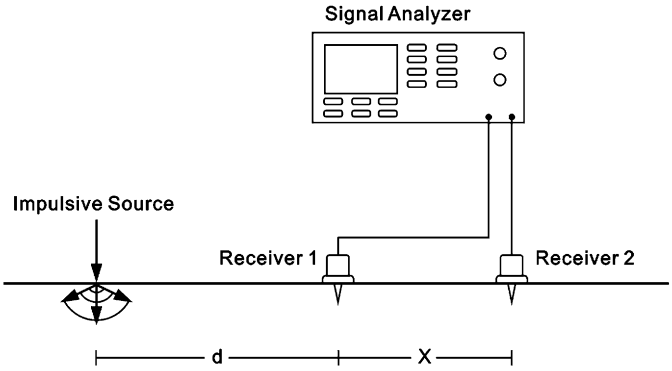

Fig. 7. Instrument configuration of the SASW method.

population of 30 individuals was generated and genetic operations were applied to generate new populations. We set the initial model as having ten layers at each site with reasonable and wide velocity ranges so that the GA could be calculated completely depending on the dispersion curve of the phase velocity and to avoid any contrived restriction. The iterations were terminated at the 500th generation, because of no further significant reductions in misfit. We used two genetic operations called crossover and mutation to generate populations and avoid localized minimum.

3.1.3. Conventional surface waves inversion

After performing the GA search to forward shear-wave velocity structures, we used a conventional surface wave inversion method (SURF) [20] to invert the more accurate shear-wave velocity structures by fitting dispersion curves. By this method, we add parameters such as densities and Poisson's ratios to constrain the models, and by doing so obtain more accurate shear-wave velocity structures.

3.2. Stress wave propagation method

3.2.1. Spectral analysis of the surface wave method

The evolution of spectral analysis of the surface wave method was from the 1980s (e.g. [9,10]), and it is a very simple, fast, efficient and widely used method to evaluate shallow shear-wave velocity structure. In this method, we estimate the relationship between phase velocity and apparent wavelengths by changing receiver positions along a straight line (Fig. 7) and using different sources. Then we obtain the phase-velocity dispersion curve of the Rayleigh wave. Rayleigh wave wavelengths (λ) are calculated by relating the space of the seismometers (X) and phase angle (θ) determined from the cross-power spectra between the seismometers [21]:

$$\lambda = \frac{2\pi X}{\theta} \tag{4}$$

The Rayleigh wave velocity is calculated as the product of the frequency and its associated wavelength:

$$V_R = \lambda f \tag{5}$$

3.2.2. Impulse response method

The IR method was proposed by the French National Construction Industry Research Center in the late 1960s. We receive the impulse signal and acceleration records via the recorder and then convert these data to a frequency domain using the Fast Fourier Transform (FFT). After dividing the acceleration spectrum ($a(\omega)$) by the impulse spectrum ($P(\omega)$), we get the transfer function of the site:

$$\text{Transfer function} = \left|\frac{a(\omega)}{P(\omega)}\right| \tag{6}$$

Chang [22] verified that the SASW method was sensitive to the shear-wave velocity of layers and the IR method was sensitive to the thickness of the layers.

The SWPM integrates the dispersion curve of the SASW method and the transfer function of the IR method and uses a forwarding manual trial and error method to evaluate the shear-wave velocity structure. Fig. 8 shows an example of the dispersion curve from the SASW method and the transfer function from the IR method.

3.3. Suspension PS-logging method

In general, there are several traditional logging methods, which include cross-hole, up-hole and down-hole velocity logging methods, denominated according to their respective locations of source and receiver. The suspension PS-logging system is different from these traditional methods in that its source and receivers are integrated and close to each other. Thus, the suspension PS-logging system can conduct continuous measurement and accuracy is better than that of the traditional methods [23]. Suspension PS-logging has two receivers at a fixed distance of 1 m. They both receive the signal produced by the source at different times so that we can pick out the first arrival of P- and S-waves and calculate the velocities of the layers (Fig. 9):

$$V_{PZ} = \frac{1}{(t_{P1} - t_{P2})}, \quad V_{SZ} = \frac{1}{(t_{S1} - t_{S2})} \tag{7}$$

The t_{P1} and t_{S1} were the first arrival times of the lower receiver. The t_{P2} and t_{S2} were the first arrival times of the upper receiver. V_{PZ} and V_{SZ} are the P-wave and S-wave velocities at depth Z.

4. Results and discussion

These important results are all shown in Figs. 10 and 12. We will discuss the shear-wave velocity structures in the top 50 or 100 m in the following paragraphs in order to compare the results of the three different methods and prove that array measurement of microtremors is also efficient in the shallow subsurface.

In the following, we will compare the shear-wave velocity structures. We use two indices to help us quantify the divergence of these results: (1) Vs_{30}; (2) the relation between the depth and the travel time of the S-wave. We

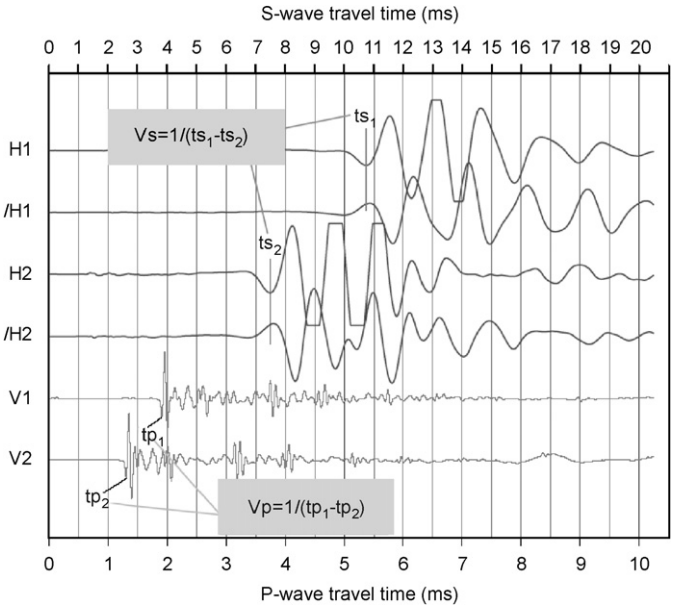

Fig. 9. Illustration of the suspension PS-logging method. V1 and V2 are the waveforms of the P-wave recorded by the upper and lower receivers. H1 and H2 are the waveforms of the S-wave recorded by the upper and lower receivers, respectively. /H1 and /H2 are also the waveforms of the S-wave, but in the opposite direction to H1 and H2.

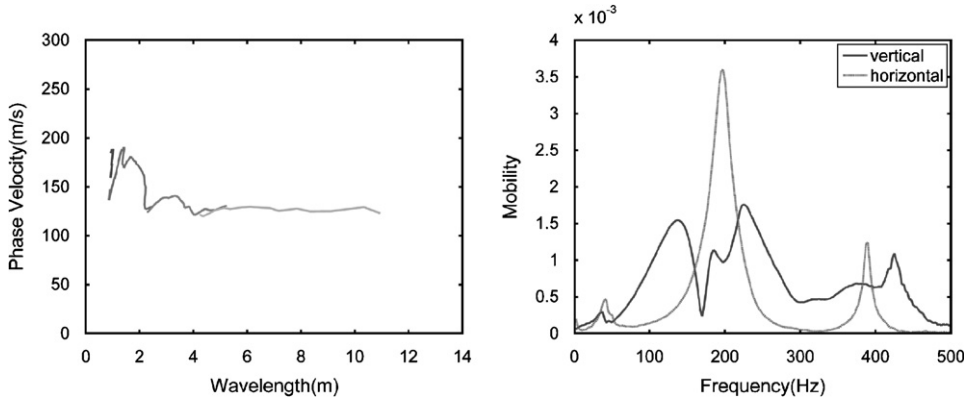

Fig. 8. Dispersion curve of ILA003 (left). Transfer functions of vertical and horizontal components (right) of ILA003.

calculated Vs_{30} by the formula

$$Vs_{30} = \frac{30}{\sum_{i=1}^{n}(Z_i/Vs_i)} \quad (8)$$

Here, Z_i and Vs_i are the thickness and the shear-wave velocity of the ith layer. The relation between the depth and the travel time of the S-wave in Ila are displayed in Figs. 11 and 13. We calculated Vs_{100} by changing the depth in formula (8) to 100 m additionally for the sites with borehole depth more than 100 m. Vs_{30} and Vs_{100} are given in Table 2 (nomenclature: the letters *a*, *p* and *s* indicate the method of microtremor array, PS-logging and SWPM, respectively). Since we consider that the shear-wave velocity structures of the three different methods are similar, we are convinced that the Vs_{30} and Vs_{100} of the structures are also comparable. In the stations with borehole depth of less than 30 m, we take the shear velocity of the deepest layer as the constant velocity in the following depth to 30 m, as the shear-wave velocity should not have severe variation at depth.

Table 2
Vs_{30} and Vs_{100} of different methods from Formula (8)

Site	Vs_{30a}	Vs_{30p}	Vs_{30s}	Vs_{100a}	Vs_{100p}
ILA003	218.5	265.6	204.7	314.4	309.3
ILA005	200.9	237.2	192.9	–	–
ILA013	201.1	194.5	269.0	–	–
ILA029	210.7	187.0	162.1	–	–
ILA041	194.1	194.2	171.8	282.6	261.9
ILA042	207.2	213.2	221.6	–	–
ILA044	195.9	159.0	179.2	–	–

Vs_{30a} defines the Vs_{30} of the microtremor array, Vs_{30p} the Vs_{30} of PS-logging, Vs_{30s} the Vs_{30} of SWPM, Vs_{100a} the Vs_{100} of microtremor array and Vs_{100p} the Vs_{100} of PS-logging. The units of Vs_{30} and Vs_{100} are both meters per second (m/s).

4.1. Borehole depth larger than 100 m

We estimated one-dimensional underground shear-wave velocity structure using the three different methods in Fig. 10. The thick dashed line is the result of microtremor array, the thin twisting line is the result of PS-logging and the thin dashed line is the result of SWPM. We got deep borehole data at more than 100 m from sites ILA003 and ILA041.

At ILA003 the $Vs_{30a} = 218.5$ m/s, $Vs_{30p} = 265.6$ m/s and $Vs_{30s} = 204.7$ m/s. We note that the value of Vs_{30a} is close to Vs_{30s}, and both are lower than Vs_{30p}. We also note at ILA003 from Fig. 11 that the S-wave travel time of the microtremor array and PS-logging are identical at a depth of about 90 m so that the Vs_{100a} (314.4 m/s) and Vs_{100p} (309.3 m/s) are also very approximate. This indicates that the average shear-wave velocity of the microtremor array and PS-logging are almost identical at a depth of 90 m. At ILA041 the Vs_{30} and Vs_{100} from the different methods (Table 2) are almost equal, and site ILA041 in Fig. 11 shows only a small divergence among the three methods. This means we have very good agreements for the shear-wave velocity structures of the three different methods at ILA041, both in the shallower part (30 m) and at depth (100 m).

4.2. Borehole depth smaller than 100 m

There are five boreholes shallower than 100 m. They are ILA029, ILA013, ILA005, ILA042 and ILA044 from north to south in Fig. 1, respectively. In order to compare the results of the three methods, we also show the one-dimensional shear-wave velocity structures and S-wave travel time curves in Figs. 12 and 13.

At ILA029, the shear-wave velocity of the SWPM was lower than both that of PS-logging and the microtremor

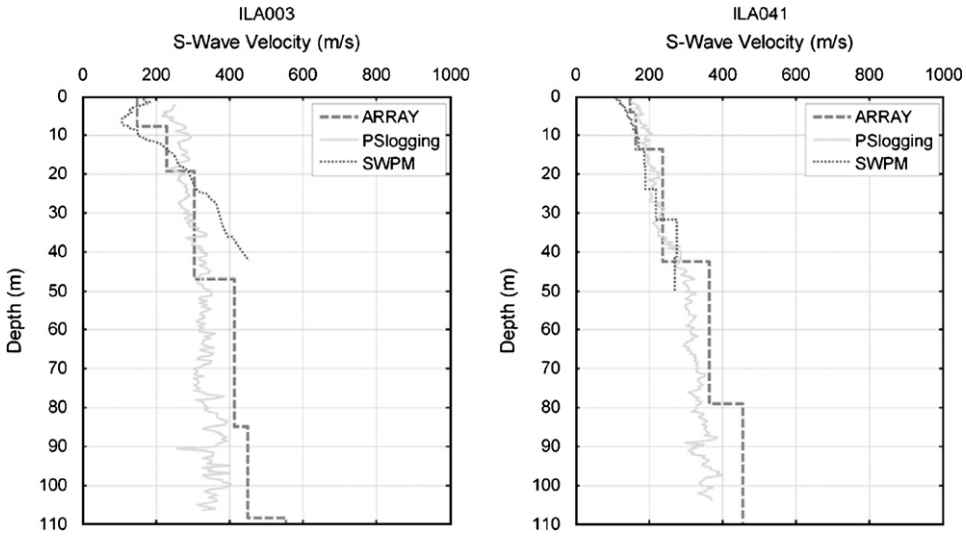

Fig. 10. One-dimensional shear-wave velocity structures of the three different methods. The borehole depths are larger than 100 m at the two sites. The thick dashed line is given by the microtremor array, the thin twisting line by PS-logging and the thin dashed line by SWPM.

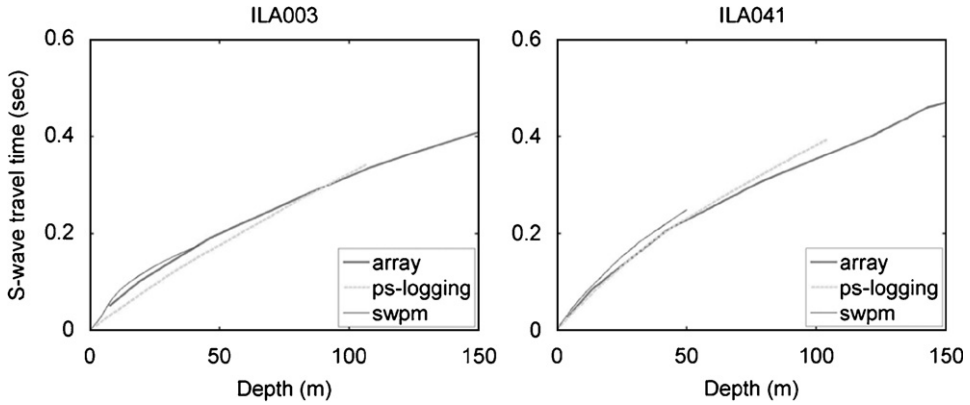

Fig. 11. The curves of depth versus travel time of S-waves from the three different methods. The thick line represents the microtremor array, the thick dashed line the PS-logging and the thin line the SWPM.

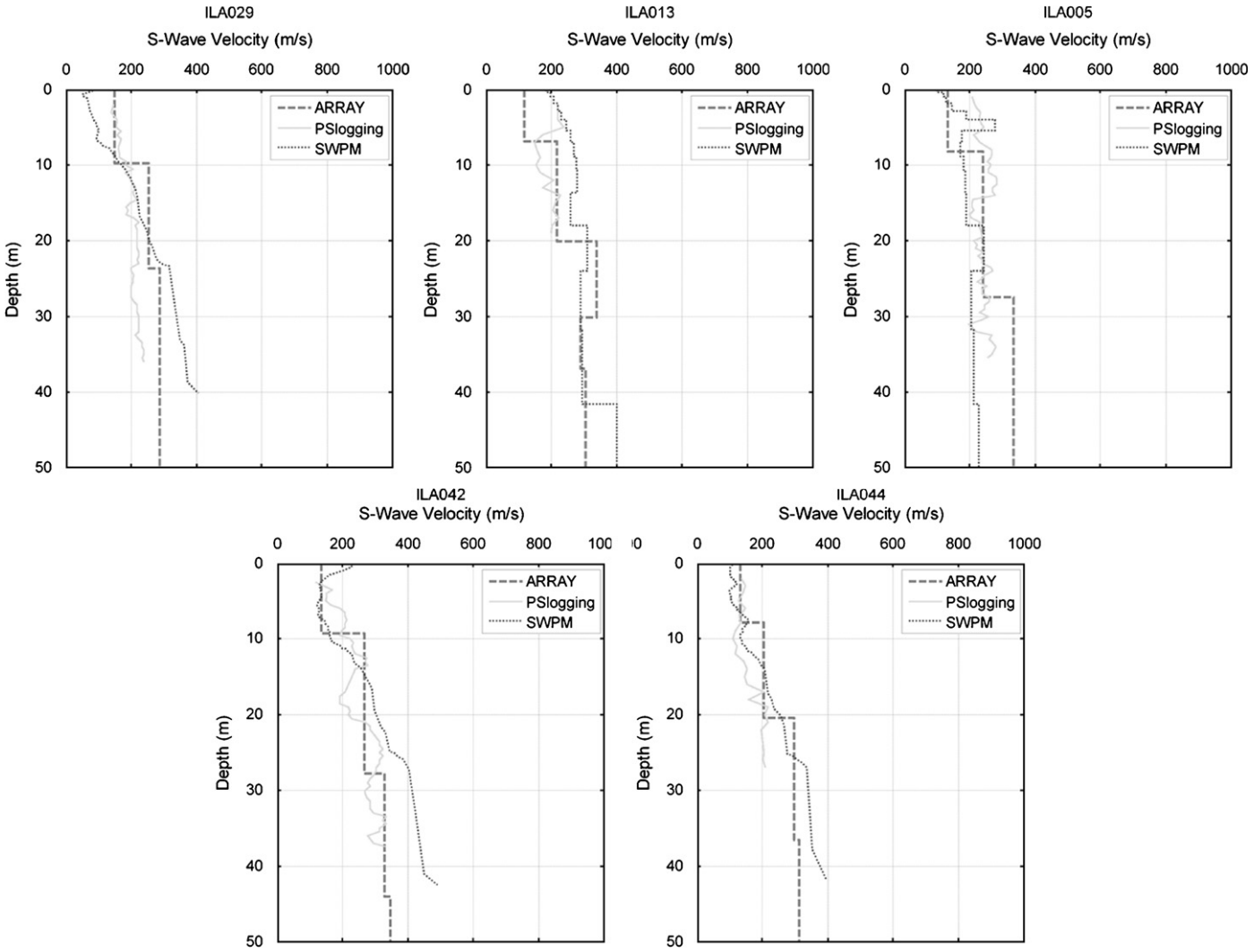

Fig. 12. One-dimensional shear-wave velocity structures of the three different methods. The borehole depths are smaller than 100 m in the five sites. The thick dashed line is given by the microtremor array, the thin twisting line by PS-logging and the thin dashed line by SWPM.

array at depths shallower than 8 m and then became higher than these two methods at depths deeper than 24 m. The divergence in the S-wave travel-time curves of the PS-logging and microtremor array methods was still acceptable. The travel-time curve of the SWPM tends toward that of PS-logging and the microtremor array in Fig. 13. This means that the average velocities of the three different methods should approach one another.

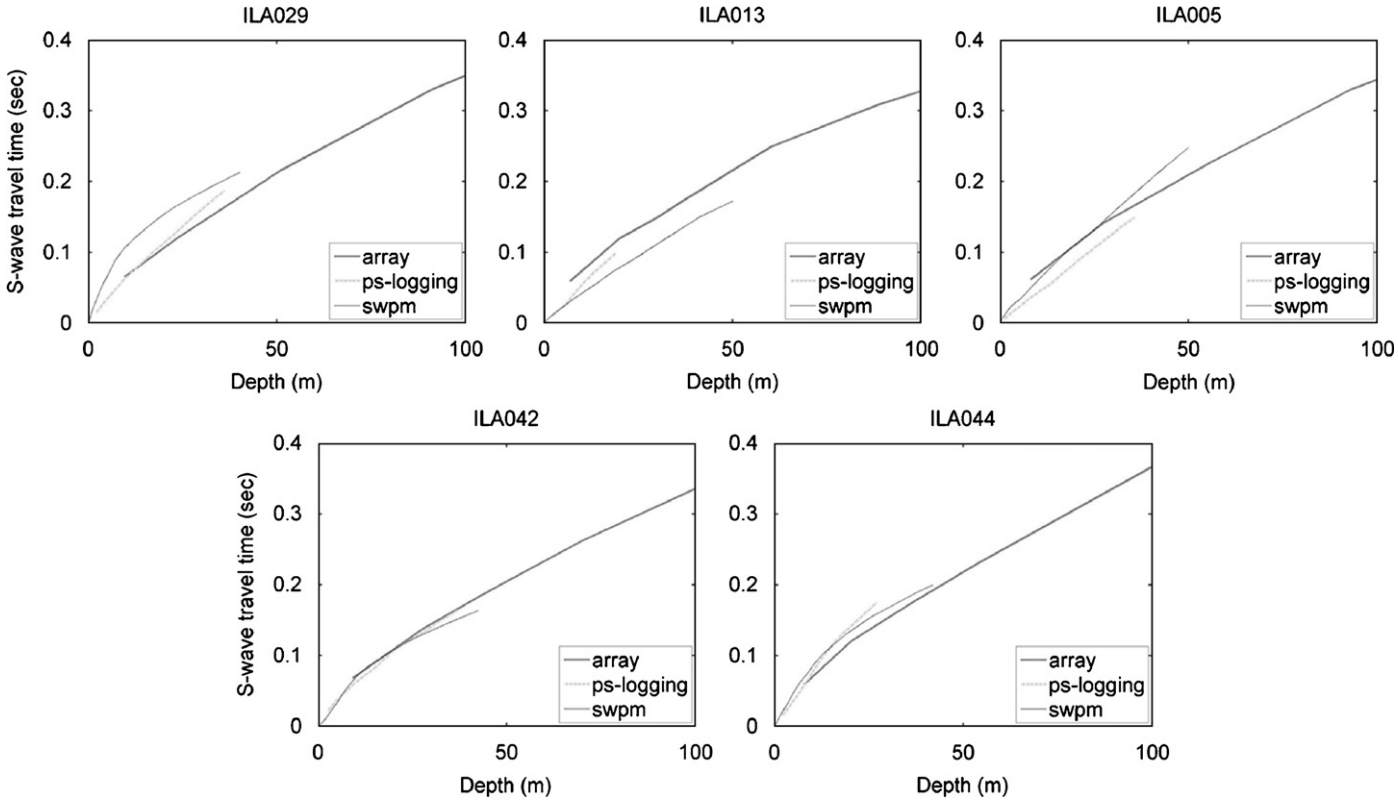

Fig. 13. The curves of depth versus travel time of S-waves from the three different methods. The thick line represents the microtremor array, the thick dashed line the PS-logging and the thin line the SWPM.

PS-logging was conducted at a depth of less than 20 m at ILA013, but the profile was close to that of SWPM and microtremor array at depths above and below 5 m. Further, the travel-time curve of PS-logging tends toward that of the microtremor array in Fig. 13. Therefore, Vs_{30p} (194.5 m/s) is close to Vs_{30a} (201.1 m/s). The shear-wave velocities of the three methods were in good agreement except for the microtremor array at depths of less than 5 m.

The degree of fit of the shear-wave velocity structure between PS-logging and the SWPM seems better than that of PS-logging and microtremor array or the SWPM and microtremor array by sight at ILA005 (Fig. 12). However, the Vs_{30a} (200.9 m/s) is closer to Vs_{30s} (192.9 m/s) than to Vs_{30p} (237.2 m/s). This is also apparent in Fig. 13. This is why we used the Vs_{30} and travel-time curve to help distinguish whether the degree of fit was good or not.

There was very good agreement between all the three methods at depths within 30 m at ILA042. The Vs_{30} (Table 2) and the S-wave travel-time curves (Fig. 12) also show this phenomenon, and, further, there was little divergence between the SWPM and the other methods at depths of more than 30 m.

At ILA044, the S-wave velocities of the three methods were also very similar at a depth of less than 20 m and the microtremor array and SWPM were still approximate at greater depths (Fig. 12). Therefore, the travel-time curves of the microtremor array and the SWPM as well as the Vs_{30a} (195.9 m/s) and Vs_{30s} (179.2 m/s) clearly began to approach each other (Fig. 13).

From the comparisons above, it is apparent that shear-wave velocity structures were not very close to each other at all sites. In Table 2, we find that the maximum difference between Vs_{30s} and Vs_{30a} was 67.9 m/s at ILA013, but between Vs_{30p} and Vs_{30a} it was only 6.6 m/s at the same site. The same phenomenon also appeared at ILA003 and ILA005. The difference between Vs_{30p} and Vs_{30s} was 60.9 m/s, but that of Vs_{30a} and Vs_{30s} was only 13.8 m/s at ILA003; while the difference between Vs_{30p} and Vs_{30a} was 36.3 m/s, but that of Vs_{30a} and Vs_{30s} was only 8.0 m/s in ILA005. This phenomenon indicates that there are at least two shear-wave velocity structure readings in good agreement even if the third is very different. From the S-wave travel-time curves (Figs. 11 and 13) we can note that there are at least two curves very closely aligned to each other at certain depths. Because maximum and minimum differences are not always attributable to the same method and the ever-present likelihood of random occurrence, we consider the larger differences as acceptable events and attribute discrepancies to the real possibility of there being a lateral heterogeneous nature to sediments at the sites.

As mentioned, we believe misfits are mainly caused by the lateral heterogeneous nature of the sediment layers. Much of this is readily attributable to differences in the methods used in measuring shear and average shear-wave

velocities; that is, the PS-logging method is based on one-dimensional measurement, SWPM on two-dimensional profiling, and the microtremor array method on a three-dimensional zone. Consequently, estimated shear-wave velocity structures would naturally have divergences when there are heterogeneous sediments.

Let us revisit the single-station horizontal-to-vertical spectra of ILA005 in Fig. 4. In the small array, the fluctuations of the H/V spectra are all in good agreement in the frequency range of 0.8–9.5 Hz used in this study. In the large array, the fluctuations of R01, R13, R14 and R15 were still in good agreement as R01 was at the center and the other three instruments were in the inner circle (radius was about 16 m). The H/V spectra of the middle circle (radius was about 32 m) at R07, R08 and R09 exhibit greater differences than that of the inner circle and the H/V spectra in the large circle (radius was about 60 m) are even more different from that of the inner circle, middle circle and from each other at frequencies higher than 3 Hz. We consider these irregularities to demonstrate the significant effect lateral variation in the shallow subsurface sediments has on measurements because irregularities increased with distance. Therefore, whilst there were some misfits in the shear-wave velocity structures from the three methods; we think they were all credible. Moreover, the average shear-wave velocity structures of the microtremor array methods may be more appropriate to describe the shear-wave velocity structures in the whole site area.

5. Conclusions

The objective of this paper is to compare the shear-wave velocity structures of three different methods and to verify the skill of the microtremor array method in the shallower sedimentary layers. The CWB and NCREE launched a project to build an engineering geological database using strong-motion stations in 2000. In this project, they measure shear-wave velocity using the suspension PS-logging method. In some of these free field strong-motion stations, we conducted array measurements of microtremors and SWPM experiments that combine the SASW and IR methods.

The SWPM utilizes a hammer at the surface to create an artificial source. The signal is measured by accelerometers at different distances from each other, in the case of our experiment 2, 4, 8, 16, and 32 m at each site. This method is extremely accurate in measuring shear-wave velocity structures in the top 40–50 m of the sediment. In recent years, suspension PS-logging has become a very popular method for measuring shear-wave velocity structures as it can measure both P-wave and S-wave velocity accurately and continuously. PS-logging measurement can be conducted successfully in borehole at a depth of up to 300 m. Previously, the microtremor array method has been used to estimate shear-wave velocity structure at depths ranging from hundreds of meters to several kilometers depending on the maximum diameter of the array; however, in this study, we attempted to evaluate the shear-wave velocity structure in the top 100 m using this method.

In most stations, the results of these methods seem similar (Figs. 10 and 12) and small misfits are acceptable. In our opinion, part divergence between the models is likely caused by lateral variations in subsurface structures. The discrepancies, whilst duly noted, probably belong to a combination of lateral variations in subsurface structures and the nature of the models used to capture shear-wave velocity. PS-logging is measured in boreholes; the SWPM estimates the average shear-wave velocity along a survey line; and the microtremor array evaluates average shear-wave velocity in a circular area; therefore, any heterogeneity would cause misfits. Of course the local geology or subsurface topography also will affect the evaluated profiles. Given this is the likely case, the misfits are acceptable and the average shear-wave velocity structures of the microtremor array method represent well the shear-wave velocity structures for the whole site region more so than the PS-logging and SWPM results do.

According to previous studies, the PS-logging method and SWPM are both considered reliable methods [21,22] for measuring shear-wave velocity structures in the shallower layers. Our study has shown that the microtremor array method can produce compatible results in these layers. The three different methods have their own virtues. The microtremor array method takes less than 4 h and needs only three people, and it can accurately evaluate shear-wave velocity structures in the surface layers and at a depth much greater than 100 m. The PS-logging method, on the other hand, is expensive and takes time, but it can calculate both the P-wave and S-wave velocity precisely and continuously. The SWPM takes less time than either of the other methods and is very accurate, but it is limited to evaluating velocity structures at the surface.

Acknowledgments

We are very grateful to the Central Weather Bureau (CWB) and the National Center for Research on Earthquake Engineering (NCREE) for providing the financial support for our measurements with the microtremor array method, PS-logging and SWPM.

References

[1] Liu HP, Boore DM, Joyner WB, Oppenheimer DH, Warrick RE, Zhang W, et al. Comparison of phase velocities from array measurements of Rayleigh waves associated with microtremor and results calculated from borehole shear-wave velocity profiles. Bull Seismol Soc Am 2000;90(3):666–78.

[2] Garcia-Jerez A, Navarro M, Alcala FJ, Luzon F, Perez-Ruiz JA, Enomoto T, et al. Shallow velocity structure using joint inversion of array and h/v spectral ratio of ambient noise: the case of Mula town (SE of Spain). Soil Dyn Earthquake Eng 2007;27:907–19.

[3] Parolai S, Picozzi M, Richwalski SM, Milkereit C. Joint inversion of phase velocity dispersion and H/V ratio curves from seismic noise recordings using a genetic algorithm, considering higher modes. Geophys Res Lett 2005;32(1):L01303.

[4] Di Giulio G, Cornou C, Ohrnberger M, Wathlet M, Rovelli A. Deriving wavefield characteristics and shear-velocity profiles from two-dimensional small-aperture arrays analysis of ambient vibrations in a small-size alluvial basin, Colfiorito, Italy. Bull Seismol Soc Am 2006;96(5):1744–55.
[5] Maresca R, Galluzzo D, Pezzo ED. H/V spectral ratios and array techniques applied to ambient noise recorded in the Colfiorito basin, central Italy. Bull Seismol Soc Am 2006;96(2):490–505.
[6] Arai H, Tokimatsu K. S-wave velocity profiling by inversion of microtremor H/V spectrum. Bull Seismol Soc Am 2004;94(1):53–63.
[7] Arai H, Tokimatsu K. S-wave velocity profiling by joint inversion of microtremor dispersion curve and horizontal-to-vertical (H/V) spectrum. Bull Seismol Soc Am 2005;95(5):1766–78.
[8] Louie JN. Faster, better: shear-wave velocity to 100 m depth from refraction microtremor arrays. Bull Seismol Soc Am 2001;91(2): 347–64.
[9] Heisey JS, Stokoe KHII, Meyer AH. Moduli of pavement systems from spectral analysis of surface waves. Transp Res Rec 1982;852: 22–31.
[10] Nazarian S, Stokoe KH II. In situ shear wave velocities from spectral analysis of surface waves. Proc 8th Conf Earthquake Eng 1984; 3:31–8.
[11] Satoh T, Kawase H, Matsushima S. Estimation of S-wave velocity structures in and around the Sendai basin, Japan, using array records of microtremors. Bull Seismol Soc Am 2001;91(2):206–18.
[12] Aki K. Space and time spectra of stationary stochastic waves, with special reference to microtremors. Bull Earthquake Res Inst 1957;35: 415–56.
[13] Capon J. High-resolution frequency–wavenumber spectrum analysis. Proc IEEE 1969;57(8):1408–18.
[14] Horike M. Inversion of phase velocity of long-period microtremors to the S-wave-velocity structure down to the basement in urbanized areas. J Phys Earth 1985;33:59–96.
[15] Matsushima T, Okada H. Determination of deep geological structures under urban areas using long-period microtremors. ButsuriTansa 1990;43:21–33.
[16] Sato T, Kawase H, Matsui M, Kataoka S. Array measurement of high frequency microtremors for underground structure estimation. Proc Fourth Int Conf Seismic Zonation 1991;2:409–16.
[17] Malagnini L, Rovelli A, Hough SE, Seeber L. Site amplification estimates in the Garigliano valley, central Italy, based on dense array measurements of ambient noise. Bull Seismol Soc Am 1993;83:1744–55.
[18] Kawase H, Satoh T, Iwata T, Irikura K. S-wave velocity structure in the San Fernando and Santa Monica areas. Proc Second Int Symp Eff Surf Geol Seismic Motions 1998;2:733–40.
[19] Kudo K, Kanno T, Okada H, Özel O, Erdik M, Sasatani T, et al. Site-specific issues for strong ground motions during the Kocaeli, Turkey, earthquake of 17 August 1999, as inferred from array observations of microtremors and aftershocks. Bull Seismol Soc Am 2002;92(1):448–65.
[20] Herrmann RB. Computer program in seismology, vol. 4. Saint Louis University; 1987.
[21] Kolsky H. Stress waves in solids. New York: Dover Publications; 1963. 143pp.
[22] Chang LC. Study of site frequency characteristics with integrated stress wave propagation method. Master thesis, National Central University, Taoyuan, Taiwan, 2002.
[23] Chen MH, Wen KL, Loh CH. A study of shear wave velocities for alluvium deposits in southwestern Taiwan. J Chin Inst Civ Hydraul Eng 2003;15(4):667–77.